Journal of Materials Chemistry C

Efficient Flash Memory Devices Based on Non-Conjugated Ferrocene-Containing Copolymers

Journal:	*Journal of Materials Chemistry C*
Manuscript ID	xxxxxxxxxxxxxxxxxxxxxx
Article Type:	Paper
Date Submitted by the Author:	n/a

Complete List of Authors:	Xiang, Jing; Department of Chemistry and Institute of Advanced Materials, Hong Kong Baptist University Li , Xiangling ; Nanjing University of Posts and Telecommunications Ma, Yun; Nanjing University of Posts and Telecommunications, Institute of Advanced Materials Zhao, Qiang; Nanjing University of Posts and Telecommunications, Institute of Advanced Materials Ho, Cheuk-Lam; The Hong Kong Polytechnic University, Department of applied biology and chemical technology Wong, Wai-Yeung (Raymond); The Hong Kong Polytechnic University, Faculty of Applied Science and Textiles

Journal of Material Chemistry C

ARTICLE

Efficient flash memory devices based on non-conjugated ferrocene-containing copolymers

Jing Xiang,[a] Xiangling Li,[b] Yun Ma,[b] Qiang Zhao,*[b] Cheuk-Lam Ho,*[a,c] Wai-Yeung Wong*[a,c]

A series of non-conjugated ferrocene-containing copolymers **FcCP1–FcCP3** with triphenylamine (TPA), benzothiazole (BT) or phenothiazine (PHZ) unit have been designed and synthesized via a facile radical polymerization protocol. The structural, photophysical, electrochemical and memory characteristics of these polymers were systematically studied. All the copolymers exhibited flash memory behaviour with a bistable conductive process, where **FcCP1** showed a large ON/OFF current ratio of 10^3 to 10^4 with a low threshold voltage of −0.6 V. Such remarkable results suggest that non-conjugated ferrocene-containing copolymers are promising active materials for memory applications.

1. Introduction

With the rapid development of information technology, novel functional materials for memory devices have attracted considerable attention in the industrial and academic communities.[1–3] As conventional memory devices comprising of inorganic semiconductors like Si, Ge and GaAs have been facing increasing challenges on downscaling and physical limitations, there is a strong desire to explore organic materials for memory application.[4–7] Particularly, organic memory devices based on polymers show promising prospects due to their remarkable features such as simple manufacturing process, high device flexibility and large-scale thin-film formation.[8–11] In the past few decades, great progress has been made in polymeric memory systems,[12–16] and several different mechanisms including charge transfer,[17–27] filamentary conduction,[28–35] space charge-limited current,[36, 37] conformational change[38, 39] as well as redox switch[40, 41] have been well established to understand the data storage behaviours.

[a] *Institute of Molecular Functional Materials, Department of Chemistry and Institute of Advanced Materials, Hong Kong Baptist University, Waterloo Road, Kowloon Tong, Hong Kong, PR China.*
[b] *Key Laboratory for Organic Electronics & Information Displays(KLOEID) and Institute of Advanced Materials (IAM), Nanjing University of Posts & Telecommunications (NUPT), 9 Wenyuan Road, Nanjing 210023, PR China.*
E-mail: iamqzhao@njupt. edu.cn
[c] Department of Applied Biology and Chemical Technology, The Hong Kong Polytechnic University, Hung Hom, Hong Kong, P. R. China
E-mail: wai-yeung.wong@polyu.edu.hk;cheuk-lam.ho@polyu.edu.hk

Due to the unique electrochemical stability of ferrocene, ferrocene-containing polymers have been widely applied for biosensors,[42, 43] liquid crystals,[44, 45] magnetic ceramics,[46–49] burning rate catalysts,[50, 51] surface modification agents[52] and organic cathodes.[53, 54] However, polymeric memory devices fabricated with ferrocene-containing materials are rarely reported. Most recently, Guan and co-workers synthesized a series of ferrocene-terminated hyperbranched polyimides (HBPI-Fcs), and the memory device with a configuration of indium tin oxide (ITO)/HBPI-Fcs/Al exhibited bistable electrical conductivity and nonvolatile bipolar write-once-read-many-times memory character. The device also showed an ON/OFF current ratio of 10^4 under a constant bias of −1.0 V and the ON/OFF stability of 10^4 s during the test period. The revealed electrical bistability of HBPI-Fcs was found to be mainly due to the charge trapping effect of the electroactive terminal ferrocene groups and the charge transfer was well fitted with the space charge-limited-current and ohmic models.[55, 56] A dual-responsive organometallic poly ionic liquid (PIL) consisting of a poly(ferrocenylsilane) backbone of a silane-bridged ferrocene unit and a tetraalkylphosphonium sulfonate moiety in the side chain was also proven to be redox responsive due to the presence of ferrocene.[57] Polyimides (PIs) containing different contents of ferrocene as the pendant group were synthesized by Qi and co-workers for electrical resistive memory device applications. Semiconductor parameter analysis indicated that the synthesized PIs possess the nonvolatile flash memory characteristic with a threshold voltage of −3.2 V. The charge transfer mechanism related to the switching effect was elucidated through molecular calculation.[58] In our previous study, four conjugated ferrocene-

containing poly(fluorenylethynylene)s have been investigated. Memory devices show flash or write-once read-many times (WORM) memory effects, and the aromatic components in the conjugated main chain play the key role in dominating the memory device performance.[59] Thus, in this work we extend our effort to design and synthesize a series of non-conjugated ferrocene-containing copolymers **FcCP1**, **FcCP2** and **FcCP3** with three different aromatic pendants for memory applications. Introduction of pendant ferrocene group could provide a redox-active switching moiety.[60] Commonly used aromatic units including electron-rich triphenylamine (TPA), hole-transporting phenothiazine (PHZ) and electron-withdrawing benzothiazole (BT) were also selected.[61–63] A facile free radical initiated polymerization was performed between vinylferrocene (**VF**) and the corresponding aromatic vinylene monomer to afford the designed copolymers **FcCP1**, **FcCP2** and **FcCP3**. Their structural, photophysical, electrochemical and memory characteristics of the resulting copolymers were systematically studied.

2. Experimental

2.1 Materials

All chemical reagents were purchased from Sigma-Aldrich, Acros Organics and Tokyo Chemical Industry Co., Ltd (TCI). All reactions were performed under a nitrogen atmosphere. The solvents used for chemical synthesis were dried and distilled by appropriate drying agents prior to use.

2.2 General procedures

NMR spectra were measured by using suitable deuterated solvents on a Bruker Ultra Shield Plus 400 MHz NMR instrument. Fourier transform infrared (FTIR) spectra were obtained on a Perkin Elmer Paragon 1000 PC spectrometer. Size exclusion chromatography (SEC) was performed on an Agilent 1050 HPLC system with visible wavelength and fluorescence detector. UV-Vis absorption spectra were measured by using a HP-8453 diode array spectrophotometer. Photoluminescence (PL) spectra were tested with a PTI Fluorescence Master Series QM1 spectrophotometer. Thermogravimetric analysis (TGA) was studied on a Perkin-Elmer TGA6 thermal analyser. Cyclic voltammetry was carried out by using a CH Instrument CV with a glassy carbon working electrode, a platinum wire auxiliary electrode and an Ag/AgCl reference electrode.

2.3 Fabrication of memory devices

The ITO glass substrates were cleaned with deionized water, acetone and ethanol for 15 min in an ultrasonic bath successively. Upon a UV-ozone treatment for 15 min, the toluene solution of each copolymer (10 mg mL^{-1}) was spin-coated onto the ITO substrate at 3000 rpm for 40 s followed by heating at 80 °C in a vacuum chamber at 10^{-5} Torr. The measured thickness of the layer was about 50 nm. Finally, aluminium top electrode with a thickness of 150 nm was thermally evaporated and deposited at a pressure of around 10^{-7} Torr through a shadow mask. Devices with an average area of about 0.3 mm^2 were obtained. The electrical and switching-time characterizations were obtained by a Keithley 2636A semiconductor parameter analyser under ambient conditions in air.

2.4 Theoretical calculations

All theoretical calculations were carried out with the Gaussian 09 package.[59] The optimization of the polymeric structures was performed using B3LYP density functional theory. The LANL2DZ basis set was used to treat the Fe atom, and the 6-31G* basis set was applied for other atoms.

3. Results and discussion

3.1 Synthesis and structural characterization

The synthetic routes for the preparation of *N, N*-bis(4-methylphenyl)-4-vinylaniline (**VM1**), 2-(4-vinylphenyl) benzo[*d*]thiazole (**VM2**) and 10-methyl-3-vinyl-10*H*-phenothiazine (**VM3**) are outlined in Scheme 1. For **VM1**, 4-di-*p*-tolylamino-benzaldehyde was firstly prepared, followed by the Wittig reaction with triphenylphosphonium ylide.[64, 65] **VM2** was obtained by the Stille coupling reaction between tributylvinyltin and 2-(4-iodophenyl) benzo[*d*]thiazole according to a modified literature procedure.[66] 10-Methyl-10*H*-phenothiazine underwent the Vilsmeier-Haack and Wittig reaction to generate **VM3**.

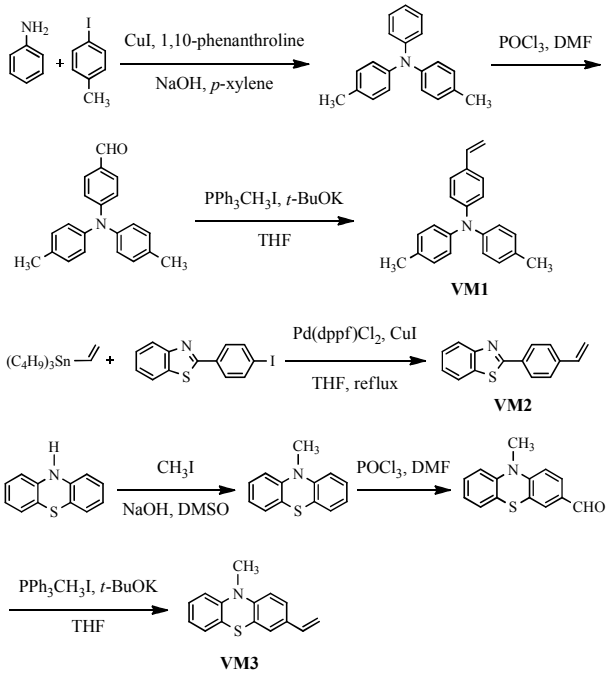

Scheme 1 Schematic representation of the synthesis of **VM1**, **VM2** and **VM3**.

As shown in Scheme 2, free radical initiated polymerization between all these synthesized vinyl-functionalized monomers and vinylferrocene was respectively carried out by using 2,2'-azobis(isobutyronitrile) (AIBN) as the initiator to afford the corresponding copolymers **FcCP1–FcCP3**.[67]

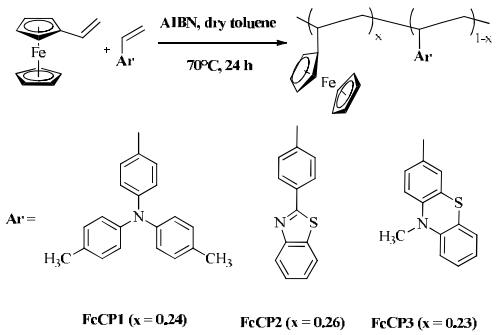

Scheme 2 Schematic representation of the synthesis of **FcCP1**, **FcCP2** and **FcCP3**.

The structures of non-conjugated ferrocene-containing copolymers were characterized by ^{1}H NMR spectroscopy. All signals in the ^{1}H NMR spectra are consistent with the corresponding structures. The broad proton signal at δ = 3.50–5.00 ppm is assigned to the ferrocene unit, while peaks at δ = 6.00–8.00 ppm are attributed to the protons of TPA, BT and PHZ units. The proton signals at δ = 2.19 and 3.25 ppm indicate the presence of methyl group in **FcCP1** and **FcCP3** (See ESI*). The mole ratio of ferrocene unit and heteroaromatic moiety in each copolymer can be calculated from the corresponding integrations of the characteristic protons in the ^{1}H NMR spectra, and all these copolymers exhibit around 1:3 molar ratio of ferrocene to TPA, BT or PHZ. (Table S1**Error! Reference source not found.**).

The FTIR spectra of non-conjugated ferrocene-containing copolymers were obtained by using KBr pellet method (Figure S1). Taking the IR spectrum of **FcCP1** as an example, the wavenumber at 3089 cm^{-1} is the typical C-H bond stretching of ferrocene, whereas peaks at 1605–1448 and 1412 cm^{-1} are assigned to the C=C stretching signals of triphenylamine and ferrocene moieties. The peak at 1270 cm^{-1} is due to the C-N stretching, while those peaks at 1106 and 1000 cm^{-1} could be attributed to the C-C stretching of ferrocene. The C-H bending and C-Fe stretching in ferrocene are respectively located at 813 and 504 cm^{-1}.[68]

Table 1 Molecular masses and PDI of copolymers

Polymer	M_n (g mol^{-1})	M_w (g mol^{-1})	PDI (M_w/M_n)
FcCP1	1.8 × 10^4	2.1 × 10^4	1.2
FcCP2	1.3 × 10^4	1.5 × 10^4	1.1
FcCP3	6.2 × 10^3	6.8 × 10^3	1.1

The molecular weight of each copolymer was analysed by size exclusion chromatography (SEC) where the results are shown in Table 1. The weight-average molecular masses are 2.1 × 10^4, 1.5 × 10^4 and 6.8 × 10^3 g mol^{-1} for **FcCP1**, **FcCP2** and **FcCP3,** respectively. The small polydispersity index (PDI) indicates the narrow mass distribution of the synthesized copolymers.

3.2 Optical and thermal properties

The UV-Vis absorption and PL spectra of non-conjugated ferrocene-containing copolymers **FcCP1–FcCP3** were measured in THF solution and the spectra are shown in Figs. 1 and 2. All copolymers exhibit intense absorption peaks at 250 and 298 nm which are assigned to the internal molecular charge transfer and metal-to-ligand charge transfer (MLCT) of ferrocene. Compared with **FcCP1**, **FcCP2** and **FcCP3** have a broader absorption peak at around 335 nm. Similarly, copolymers **FcCP2** and **FcCP3** show an emission peak at 460 nm, while the emission signal of **FcCP1** functionalized with TPA unit is strongly blue shifted to 384 nm. The significant difference of the emission spectrum was probably resulted from the bulky TPA moiety which prevents the conjugation effect in **FcCP1**.

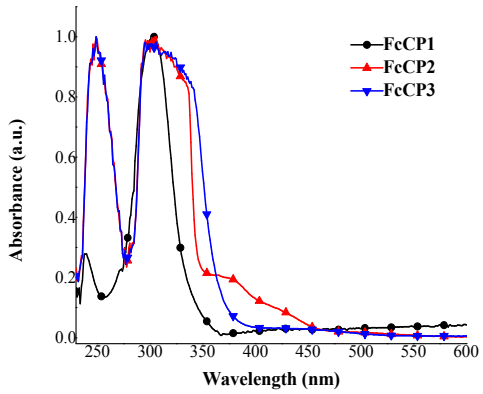

Fig. 1. Absorption spectra of the copolymers in THF solution.

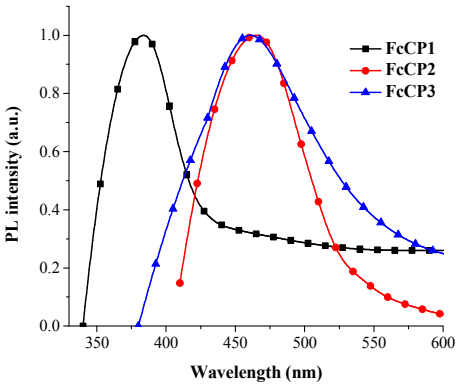

Fig. 2. PL spectra of the copolymers in THF solution

TGA of **FcCP1–FcCP3** was carried out and the corresponding decomposition temperatures (T_d) at 5% weight loss are 390, 348 and 369°C for **FcCP1**, **FcCP2** and **FcCP3**, respectively (Figure S2). The results suggest that all these non-conjugated ferrocene-containing copolymers have high thermal stability for long operating lifetime memory application.

3.3 Electrochemical properties

The electrochemical properties of the as-prepared copolymers were investigated by CV in thin film state. CV measurements of copolymer films on a glassy carbon electrode were taken in 0.1 M solution of tetrabutylammonium hexafluorophosphate (n-Bu_4NPF_6) in anhydrous acetonitrile. The ferrocene/ferrocenium couple was used as the internal standard at a scan rate of 50 mV s^{-1}. The potentials of oxidation (E_{ox}) and reduction (E_{red}) as well as energy levels of the highest occupied molecular orbital (E_{HOMO}) and the lowest unoccupied molecular orbital (E_{LUMO}) are summarized in Table 2, where the HOMO and LUMO values could be calculated by the equation of $E_{HOMO/LUMO} = (E_{Ox/Red(onset)} + 4.80)$ eV. Due to the outstanding electron-donating properties of TPA and PHZ, the E_{ox} value as well as the E_{HOMO} of **FcCP1** and **FcCP3** is much higher than that of **FcCP2**.

Table 2 Electrochemical results of **FcCP1–FcCP3** in 0.1 M n-Bu_4NPF_6 acetonitrile solution

Polymer	E_{ox}(V)	E_{red} (V)	E_{HOMO} (eV)	E_{LUMO} (eV)
FcCP1	0.46	−1.28	−5.26	−3.52
FcCP2	1.89	−1.44	−6.69	−3.36
FcCP3	0.35	−1.37	−5.15	−3.43

3.4 Characteristics of memory devices

Solution manufacturing process was applied to fabricate the memory devices of the non-conjugated ferrocene-containing copolymers. The copolymer active layer was spin-coated onto the cleaned ITO glass substrate, followed by evaporation of the aluminium (Al) on the active layer as electrode to form a sandwich structure (ITO/polymer/Al). The Al electrode and the bottom ITO electrode were connected to a tunable voltage source to study the memory effect and electrical bistability of each copolymer. The corresponding current-voltage (I-V) curve was obtained by applying a swept voltage to the device. For **FcCP1** (Fig. 3a), the device is under a low conductive state when the voltage is swept from 0 to −0.6 V. An abrupt increase in current from 10^{-5} to 10^{-2} A could be observed at the voltage of −0.6 V. The high conductive state is maintained during the subsequent negative sweep from −0.6 to −5.0 V (first sweep). This transition process from low conductivity (~10^{-5} A, OFF state, i.e. "0" signal in data storage) to high conductivity (~10^{-2} A, ON state, i.e. "1" signal in data storage) is equivalent to the ''writing'' process. The ON state is kept during the subsequent negative sweep as well as the scanning process from −5.0 to 0 V (second sweep), which corresponds to the ''reading'' process. The memory device stays in the ON state when the sweep voltage is scanned from 0 to 2.5 V. A sudden decrease of current from 10^{-2} to 10^{-5} A is occurred at around 3 V and the low current is maintained during the following scanning process from 3 to 5 V (third sweep). It indicates that the high conductive state (ON state) is returned to the low conductive state (OFF state), referred as the ''erasing'' process. The OFF state is maintained from 5.0 to 0 V upon the removal of power supply (fourth sweep). In addition, the memory device of **FcCP1** can be repeatedly written, read or erased when the switching voltages are applied again (the fifth sweep to the eighth sweep). Therefore, this device exhibits a remarkable bipolar flash memory property due to the repeatable "writing" and "erasing" process under the negative and positive scanning mode. A large ON/OFF current ratio of 10^3 to 10^4 is achieved, which allows the memory device to work with a low misreading rate. It is also found that the polymeric ITO/**FcCP1**/Al device shows a lower threshold "writing" voltage than that of the TPA-containing poly(fluorenylethynylene) device in our previous work.[59]

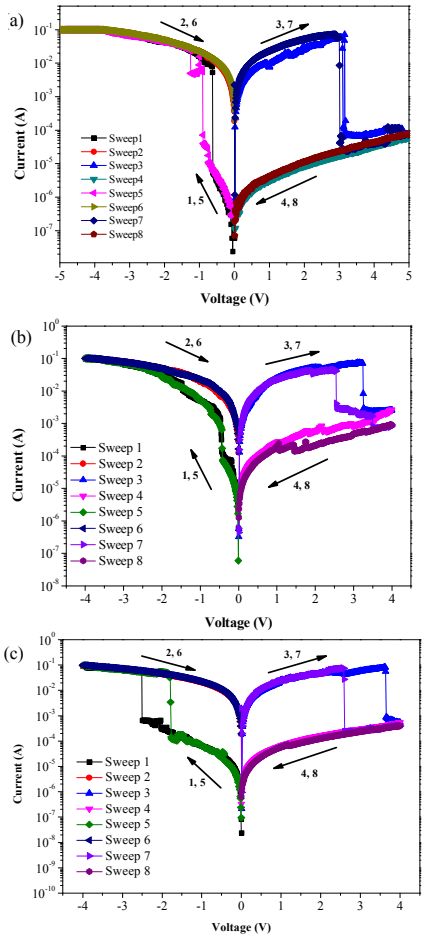

Fig. 3. Typical I–V characteristics of the ITO/polymer/Al memory devices based on copolymers (a) **FcCP1**(b) **FcCP2** and (c) **FcCP3**.

The *I–V* curves of the devices fabricated with **FcCP2** and **FcCP3** (Fig. 3b and 3c) also exhibit the similar memory behaviour to that of **FcCP1**. As to **FcCP2**, the threshold voltage for the ON state is −0.5 V with the ON/OFF current ratio is 10^2, and the memory device can be switched to the OFF state at 3.2 V. For **FcCP3**, the "writing" voltage is −2.5 V and the "erasing" voltage is 3.7 V with a ON/OFF current ratio of 10^2. The *I–V* results mentioned above show the excellent bistability of the synthesized non-conjugated ferrocene-containing copolymers **FcCP1–FcCP3**, suggesting their great potential to be applied as active materials for flash memory devices.

The retention time and stress reliability of polymeric memory devices based on **FcCP1**–**FcCP3** were measured to investigate their stability and reproductivity, and the results are summarized in Fig. 4. All the devices can keep the ON state without degradation even after 10^4 read pulses. These data suggest that the synthesized non-conjugated ferrocene-containing copolymers **FcCP1–FcCP3** exhibit a highly stable status in both ON and OFF states. The outstanding *I–V* characteristics and the excellent stability of these non-conjugated ferrocene-containing polymeric devices illustrate

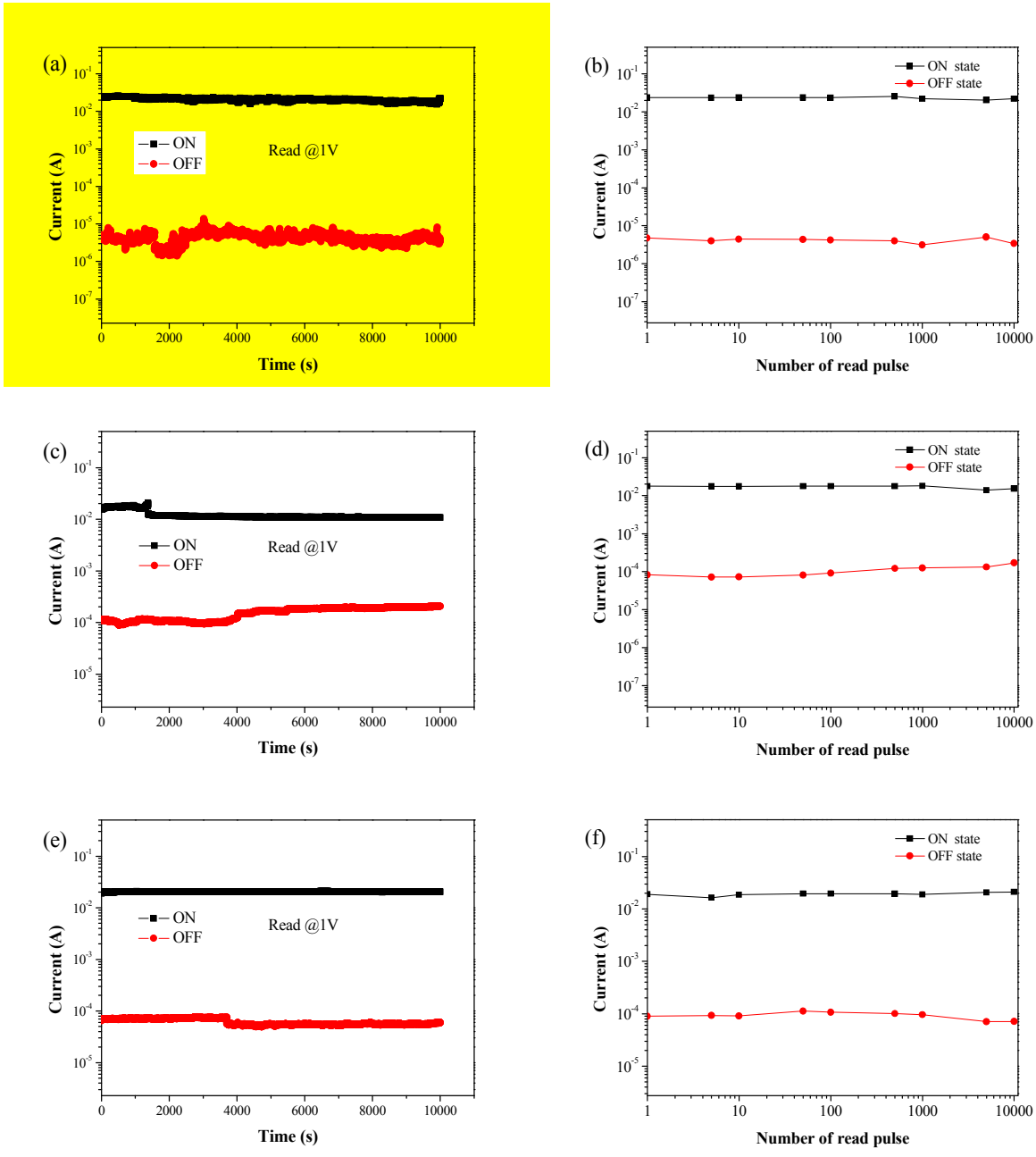

Fig. 4. Parameters of memory devices: (left) Retention time in the ON and OFF states under a constant stress of 1.0 V, (a) **FcCP1**, (c) **FcCP2**, (e) **FcCP3**; (right) Number of read pulse in the ON and OFF states under continuous read pulses of 1.0 V, (b) **FcCP1**, (d) **FcCP2**, (f) **FcCP3**.

that **FcCP1–FcCP3** are promising materials for practical rewritable memory applications.

a large driving voltage is required to switch on the memory device to a high conductive state. Therefore, memory device

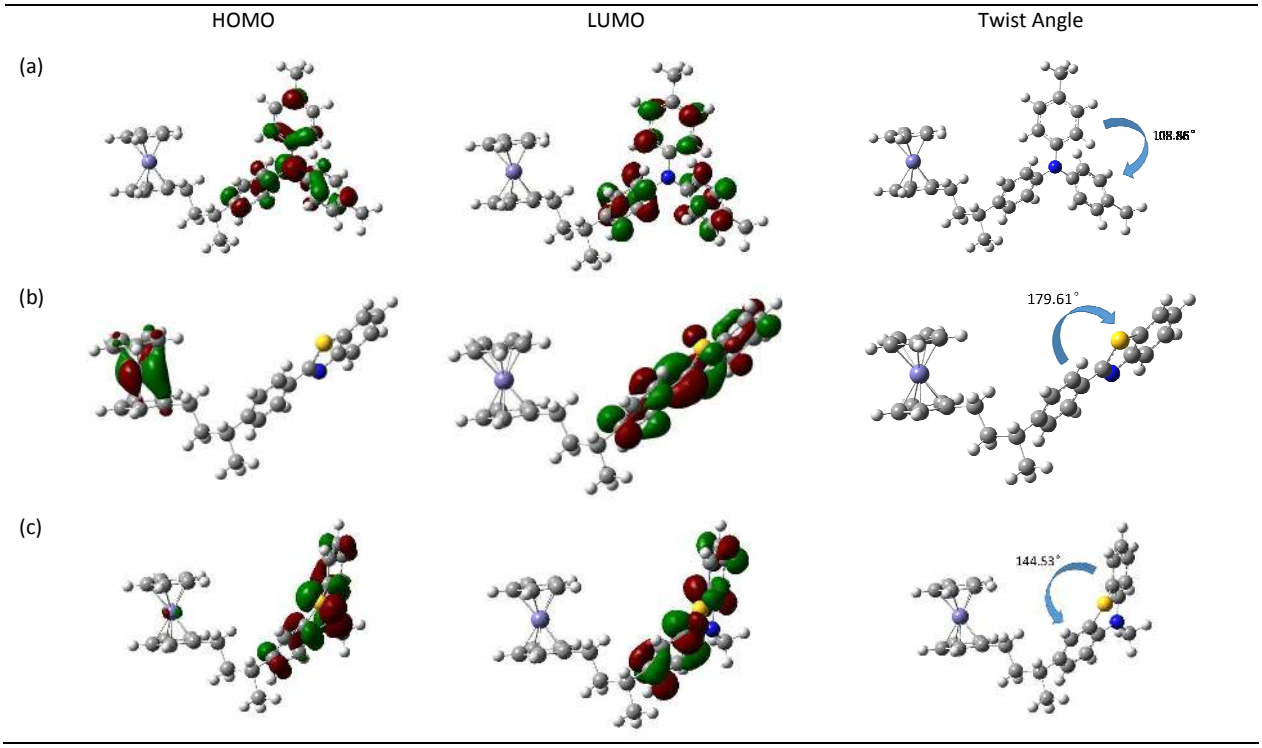

Fig. 5. Calculated HOMO, LUMO and twist angle of the model oligomers: (a) **FcCP1**; (b) **FcCP2**; (c) **FcCP3**

To further understand the variations in ON/OFF switch threshold voltages of memory devices, the HOMO and LUMO energy levels of the as-prepared **FcCP1**–**FcCP3** as well as the molecular geometries of different side units TPA, BT and PHZ were studied by DFT calculations (Fig. 5). Different from **FcCP1** and **FcCP3** in which the HOMO is entirely distributed on the TPA and PHZ units, the calculated HOMO of **FcCP2** is located on the ferrocene group, implying TPA and PHZ are more electron donating than BT, which is consistent with the CV result. Initially, all the pendant groups in **FcCP1–FcCP3** are in random orientation and the corresponding polymeric devices are under OFF state with low conductivity. When a negative bias from 0 to −4.0 V is applied, ferrocene (Fe^{2+}) could be firstly oxidized to ferrocenium ion (Fe^{3+}).[55–59] However, due to the large steric hindrance induced by the bulky TPA moiety, the intramolecular aggregation is effectively suppressed in **FcCp1**. The rigid molecular skeleton of PHZ also relieves the π–π stacking effect in **FcCP3**, while **FcCP2** with the planar BT unit (twist angle = 179.61°) favours the intrachain π–π stacking. Thus, the memory device based on **FcCP2** could be easily switched to a high conductive state via a slight conformation change, resulting in the low ON switch voltage of −0.5 V. Compared with TPA, the methyl group in PHZ and its rigid configuration provides a more significant steric hindrance, and fabricated with **FcCP3** exhibits the highest ON threshold voltage of −2.5 V. Similarly, due to the high rotational degree of three C-N bonds, the pendant TPA group allows a large free volume and a great degree of conformational freedom, and thus the polymer device based on **FcCP1** exhibits the lowest OFF switch voltage of 2.5 V when a reverse voltage from 0 to 4 V is applied. Moreover, this high rotational degree of pendant TPA also allows a significant conformational change of **FcCP1**, resulting in the highest ON/OFF ratio of 10^3 to 10^4. In this regard, the pendant units in **FcCP1**–**FcCP3** play an important role to stabilize ferrocene/ferrocenium during different scanning sweeps.

4. Conclusion

In this work, a series of non-conjugated copolymers with pendant ferrocene and different aromatic units were systematically investigated. The structural, photophysical, electrochemical and thermal properties of these copolymers were well studied. All copolymers exhibited flash memory effects with long retention time over 10^4 s and large read cycles up to 10^4. Memory device based on **FcCP1** shows an impressive *I–V* characteristic and a high ON/OFF ratio of 10^3 to 10^4 at a low threshold voltage of −0.6 V, which is superior to

the reported ferrocene-containing polymeric devices.[6, 40, 59] The device fabricated with **FcCP2** showed an extremely low threshold voltage of −0.5 V for switching on the "writing" process. These remarkable results indicate that these non-conjugated ferrocene-containing copolymers are potential active materials for non-volatile memory application.

Conflicts of interest

There are no conflicts to declare.

Acknowledgements

We are grateful to the financial support from the Hong Kong Research Grants Council (PolyU 153051/17P), National Natural Science Foundation of China (project numbers 61274018 and 21174064), Areas of Excellence Scheme, University Grants Committee of HKSAR (project No. AoE/P-03/08), Hong Kong Polytechnic University (1-ZE1C) and Ms. Clarea Au for the Endowed Professorship in Energy (847S). C. -L. Ho thanks the Hong Kong Research Grants Council (PolyU 123021/17P), National Natural Science Foundation of China (21504074) and the Hong Kong Polytechnic University (1-BE0Q) for their financial support.

Notes and references

1 W. P. Lin, S. J. Liu, T. Gao, Q. Zhao and W. Huang, *Adv. Mater.*, 2014, **26**, 570–606.
2 S. Ezugwu, J. A. Paquette, V. Yadav, J. B. Gilroy and G. Fanchini, *Adv. Electron. Mater.*, 2016, **2**, 1600253–1600262.
3 X. F. Cheng, E. B. Shi, X. Hou, J. Shu, J. H. He, H. Li, Q. F. Xu, N. J. Li, D. Y. Chen and J. M. Lu, *Adv. Electron. Mater.*, 2017, **3**, 1700107–1700115.
4 Y. Yang, J. Y. Ouyang, L. P. Ma, J. H. Tseng and C. W. Chu, *Adv. Funct. Mater.*, 2006, **16**, 1001–1014.
5 B. Cho, S. Song, Y. Li, T. W. Kim and T. Lee, *Adv. Funct. Mater.*, 2011, **21**, 2806–2829.
6 G. F. Tian, S. L. Qi, F. Chen, L. Shi, W. P. Hu and D. Z. Wu, *Appl. Phys. Lett*., 2011, **98**, 203302-1–203302-3.
7 P. Wang, S. J. Liu, Z. H. Lin, X. C. Dong, Q. Zhao, W. P. Lin, M. D. Yi, S. H. Ye, C. X. Zhu and W. Huang, *J. Mater. Chem.*, 2012, **22**, 9576–9583.
8 E. B. Shi, J. H. He, Z. Zhuang, H. Z. Liu, Y. F. Zheng H. Li Q. F. Xu, J. W. Zheng and J. M. Lu, *J. Mater. Chem. C*, 2016, **4**, 2579−2586.
9 Z. X. Zhou, L. J. Qu, T. T. Yang, J. L. Wen, Y. Zhang, Z. G. Chi, S. W. Liu, X. D. Chen and J. R. Xu, *RSC Adv.*, 2016, **6**, 52798–52809.
10 M. C. Tsai, C. L. Wang, C. Y. Lin, C. L. Tsai, H. J. Yen, H. C. You and G. S. Liou, *Polym. Chem*., 2016, **7**, 2780–2784.
11 H. J. Yen and G. S. Liou, *Polym. J.*, 2016, **48**, 117–138.
12 L. H. Xie, Q. D. Ling, X. Y. Hou and W. Huang, *J. Am. Chem. Soc.*, 2008, **130**, 2120–2121.
13 S. J. Liu, P. Wang, Q. Zhao, H. Y. Yang, J. Wong, H. B. Sun, X. C. Dong, W. P. Lin and W. Huang, *Adv. Mater.*, 2012, **24**, 2901–2905.
14 S. Rana, A. Prasoon, P. K. Jha, A. Prathamshetti and N. Ballav, *J. Phys. Chem. Lett.*, 2017, **8**, 5008–5014.
15 H. J. Yen, C. S. Shan, L. Wang, P. Xu, M. Zhou and H. L. Wang, *Polymers*, 2017, **9**, 25–40.
16 H. C. Yu, M. Y. Kim, M. Hong, K. Nam, J. Y. Choi, K. H. Lee, K. K. Baeck, K. K. Kim, S. Cho and C. M. Chung, *Electron. Mater. Lett.*, 2017, **13**, 1–8.
17 B. B. Cui, Z. P. Mao, Y. X. Chen, Y. W. Zhong, G. Yu, C. L. Zhan and J. N. Yao, *Chem. Sci*., 2015, **6**, 1308–1315.
18 Y. P. Hsiao, W. L. Yang, L. M. Lin, F. T. Chin, Y. H. Lin, K. L. Yang and C. C. Wu, *Microelectron. Reliab*., 2015, **55**, 2188–2197.
19 T. T. Huang, C. L. Tsai, S. H. Hsiao and G. S. Liou, *RSC Adv*., 2016, **6**, 28815–28819.
20 M. N. Awais, M. Mustafa, M. N. Shehzad, U. Farooq, M. T. Hamayun and K. H. Choi, *Micro Nano Lett*., 2016, **11**, 712–714.
21 Y. Kim, D. Yoo, J. Jang, Y. Song, H. Jeong, K. Cho, W. T. Hwang, W. Lee, T. W. Kim and T. Lee, *Org. Electron*., 2016, **33**, 48–54.
22 J. Zhao, L. Peng, Y. L. Zhu, Y. J. Song, L. J. Wang and Y. Z. Shen, *Polymer*, 2016, **91**, 118–127.
23 L. J. Qu, S. D. Huang, Y. Zhang, Z. G. Chi, S. W. Liu, X. D. Chen and J. R. Xu, *J. Mater. Chem. C*, 2017, **5**, 6457–6466.
24 W. Lv, H. J. Liu, W. Wang, E. Yang, H. Y. Zhen and Q. D. Ling, *RSC Adv*., 2017, **7**, 18384–18391.
25 N. F. Jia, G. F. Tian, S. L. Qi, J. H. Cheng, X. D. Wang and D. Z. Wu, *RSC Adv*., 2017, **7**, 23550–23559.
26 W. Y. Lee, H. C. Wu, C. Lu, B. D. Naab, W. C. Chen and Z. N, Bao, *Adv. Mater*., 2017, **29**, 1605166–1605172.
27 B. Zhang, L. Liu, L. X. Wang, B. Liu, X. Y. Tian and Y. Chen, *Carbon*, 2018, **134**, 500–506.
28 B. C. Jang, H. Seong, J. Y. Kim, B. J. Koo, S. K. Kim, S. Y. Yang, S. G. Im and S. Y. Choi, *2D Mater.*, 2015, **2**, 044013–044019.
29 B. C. Jang, H. Seong, S. K. Kim, J. Y. Kim, B. J. Koo, J. Choi, S. Y. Yang, S. G. Im and S. Y. Choi, *ACS Appl. Mater. Interfaces*, 2016, **8**, 12951–12958.
30 Y. Sakuragawa, Y. Takagi, T. Ikai, K. Maeda, T. T. Dao, H. Sakai and H. Murata, *Jpn. J. Appl. Phys*., 2016, **55**, 03DC10-1–03DC10-4.
31 D. H. Kang, W. Y. Choi, H. Woo, S. Jang, H. Y. Park, J. Shim, J. W. Choi, S. Kim, S. Jeon, S. Lee and J. H. Park, *ACS Appl. Mater. Interfaces*, 2017, **9**, 27073–27082.
32 P. Wang, H. L. Wang, Y. Fang, H. Li, J. H. He, Y. J. Ji, Y. Y. Li, Q. F. Xu, J. W. Zheng and J. M. Lu, *ACS Appl. Mater. Interfaces*, 2017, **9**, 32930–32938.
33 T. T. Wei, G. Chen, S. Zhang, Y. Chen, Y. T. Hu, R. Jiang and Y. X. Li, *Microelectron. Eng*., 2016, **162**, 85–88.
34 F. Fan, B. Zhang, Y. M. Cao, X. T. Yang, J. W. Gu and Y. Chen, *Nanoscale*, 2017, **9**, 10610–10618.
35 D. C. Guo, Z. Y. Sun, S. H. Wang, X. D. Bai, L. D. Xu, Q. Yang, Y. Xin, R. R. Zheng, D. G. Ma, X. F. Zhao and C. Wang, *RSC Adv*., 2017, **7**, 10323–10332.
36 B. G. Kang, J. Jang, Y. Song, M. J. Kim, T. Lee and J. S. Lee, *Polym. Chem.*, 2015, **6**, 4264–4270.
37 A. N. Cha, S. A. Lee, S. Bae, S. H. Lee, D. S. Lee, G. Wang and T. W. Kim, *ACS Appl. Mater. Interfaces*, 2017, **9**, 2730–2738.
38 Z. Li, M. Wang, H. Li, J. H. He, N. J. Li, Q. F. Xu and J. M. Lu, *J. Mater. Chem. C*, 2017, **5**, 8593–8598.
39 H. L. Wang, F. Zhou, L. X. Wu, X. Xiao, P. Y. Gu, J. Jiang, Q. F. Xu and J. M. Lu, *Polym. Chem*., 2018, **9**, 1139–1146.

40 T. L. Choi, K. H. Lee, W. J. Joo, S. Lee, T. W. Lee and M. Y. Chae, *J. Am. Chem. Soc*., 2007, **129**, 9842–9843.
41 A. Bandyopadhyay, S. Sahu and M. Higuchi, *J. Am. Chem. Soc.*, 2011, **133**, 1168–1171.
42 H. Khalid, H. J. Yu, L. Wang, W. A. Amer, M. Akram, N. M. Abbasi, Z. ul-Abdin and M. Saleem, *Polym. Chem*., 2014, **5**, 6879–6892.
43 M. Saleem, H. J. Yu, L. Wang, Z. ul-Abdin, H. Khalid, M. Akram, N. M. Abbasi and J. Huang, *Anal. Chim. Acta*, 2015, **876**, 9–25.
44 Y. Gao and J. M. Shreeve, *J. Polym. Sci. Part A Polym. Chem. Ed*., 2005, **43**, 974–983.
45 J. Brettar, T. Bürgi, B. Donnio, D. Guillon, R. Klappert, T. Scharf and R. Deschenaux, *Adv. Funct. Mater*., 2006, **16**, 260–267.
46 M. J. MacLachlan, M. Ginzburg, N. Coombs, T. W. Coyle, N. P. Raju, J. E. Greedan, G. A. Ozin and I. Manners, *Science*, 2000, **287**, 1460–1463.
47 K. Kulbaba, R. Resendes, A. Cheng, A. Bartole, A. Safa-Sefat, N. Coombs, H. D. H. Stöver, J. E. Greedan, G. A. Ozin and I. Manners, *Adv. Mater*., 2001, **13**, 732–736.
48 M. Ginzburg, M. J. MacLachlan, S. M. Yang, N. Coombs, T. W. Coyle, N. P. Raju, J. E. Greedan, R. H. Herber, G. A. Ozin and I. Manners, *J. Am. Chem. Soc*., 2002, **124**, 2625–2639.
49 K. Kulbaba, A. Cheng, A. Bartole, S. Greenberg, R. Resendes, N. Coombs, A. Safa-Sefat, J. E. Greedan, H. D. H. Stöver, G. A. Ozin and I. Manners, *J. Am. Chem. Soc*., 2002, **124**, 12522–12534.
50 Z. ul-Abdin, H. J. Yu, L. Wang, M. Saleem, H. Khalid, N. M. Abbasi and M. Akram, *Appl. Organomet. Chem*., 2014, **28**, 567–575.
51 R. B. Tong, Y. L. Zhao, L. Wang, H. J. Yu, F. J. Ren, M. Saleem and W. A. Amer, *J. Organomet. Chem*., 2014, **755**, 16–32.
52 J. Elbert, M. Gallei, C. Rüttiger, A. Brunsen, H. Didzoleit, B. Stühn and M. Rehahn, *Organometallics*, 2013, **32**, 5873−5878.
53 H. Zhong, G. F. Wang, Z. P. Song, X. Li, H. D. Tang, Y. H. Zhou and H. Zhan, *Chem. Commun*., 2014, **50**, 6768–6770.
54 J. Xiang, K. Sato, H. Tokue, K. Oyaizu, C. L. Ho, H. Nishide, W. Y. Wong and M. D. Wei, *Eur. J. Inorg. Chem*., 2016, **2016**, 1030–1035.
55 H. W. Tan, H. Y. Yao, Y. Song, S. Y. Zhu, H. X. Yu and S. W. Guan, *Dyes Pigm*., 2017, **146**, 210–218.
56 H. W. Tan, H. X. Yu, Y. Song, S. Y. Zhu, B. Zhang, H. Y. Yao and S. W. Guan, *J. Polym. Sci., Part A Polym. Chem*., 2018, **56**, 505–513.
57 K. H. Zhang, X. L. Feng, C. N. Ye, M. A. Hempenius and G. J. Vancso, *J. Am. Chem. Soc*., 2017, **139**, 10029–10035.
58 R. Hao, N. F. Jia, G. F. Tian, S. L. Qi, L. Shi, X. D. Wang and D. Z. Wu, *Mater. Des*., 2018, **139**, 298–303.
59 J. Xiang, T. K. Wang, Q. Zhao, W. Huang, C. L. Ho and W. Y. Wong, *J. Mater. Chem. C*, 2016, **4**, 921–928.
60 R. Pietschnig, *Chem. Soc. Rev*., 2016, **45**, 5216–5231.
61 B. Wang, Y. C. Wang, J. L. Hua, Y. H. Jiang, J. H. Huang, S. X. Qian and H. Tian, *Chem. Eur. J*., 2011, **17**, 2647–2655.
62 X. L. Yang, G. J. Zhou and W. Y. Wong, *Chem. Soc. Rev*., 2015, **44**, 8484–8575.
63 Z. S. Huang, H. Meier and D. Cao, *J. Mater. Chem. C*, 2016, **4**, 2404–2426.
64 Z. He, W. Y. Wong, X. M. Yu, H. S. Kwok and Z. Y. Lin, *Inorg. Chem*., 2006, **45**, 10922–10937.
65 K. P. Li, J. L. Qu, B. Xu, Y. H. Zhou, L. J. Liu, P. Peng and W. J. Tian, *New J. Chem*., 2009, **33**, 2120–2127.
66 K. D. Belfield, A. R. Morales, B. S. Kang, J. M. Hales, D. J. Hagan, E. W. V. Stryland, V. M. Chapela and J. Percino, *Chem. Mater*., 2004, **16**, 4634–4641.
67 R. J. Santos, B. G. Soares and A. S. Gomes, *Macromol. Chem. Phys.*, 1994, **195**, 2517–2521.
68 W. Z. Zhang, X. W. Kan, S. F. Jiao, J. G. Sun, D. S. Yang and B. Fang, *J. Appl. Polym. Sci*., 2006, **102**, 5633–5639.

Table of Contents

Efficient flash memory devices based on non-conjugated ferrocene-containing copolymers

Jing Xiang, Xiangling Li, Yun Ma, Qiang Zhao,* Cheuk-Lam Ho,* Wai-Yeung Wong*

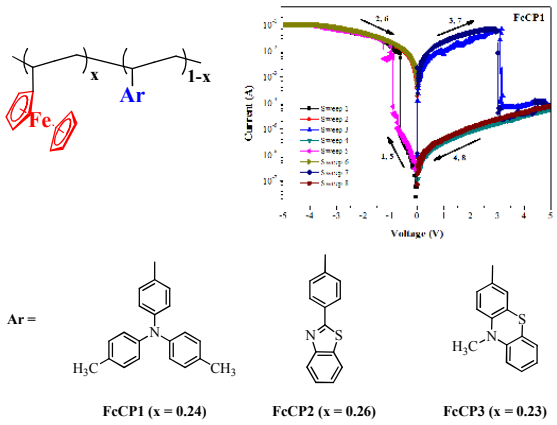

Non-conjugated ferrocene-containing copolymers **FcCP1–FcCP3** with triphenylamine, benzothiazole or phenothiazine pendant group show flash memory behaviour with a bistable conductive process. **FcCP1** showed a large ON/OFF current ratio of 10^3 to 10^4 and a low threshold voltage of −0.6 V. The different π–π stacking effects induced by the molecular geometry of **FcCP1–FcCP3** were attributed to their variations in the ON/OFF threshold voltage.